Subducting-plate Topography and Nucleation of Great and Giant Earthquakes along the South American Trench

Sara Carena
University of Munich

INTRODUCTION

It has long been recognized that the locations and geometries of large subduction zone thrust earthquakes are influenced by features on the subducting plate (Mogi 1969; Vogt *et al.* 1976; Kelleher and McCann 1976; Cloos 1992; Bilek 2007; Das and Watts 2009). This phenomenon is particularly evident along the South American trench, where the recent 27 February 2010 M_w 8.8 Maule, Chile, earthquake is the latest in a series of six events larger than M_w ~ 8.5 that have occurred along the trench since 1900 (Table 1). A striking feature of these events, as well as of older, pre-instrumental ones whose epicenter locations can be reasonably estimated, is that their epicenters are located near the intersection of an oceanic fracture zone on the Nazca plate with the trench (Figures 1 and 2). Some of these events have previously been associated with ridges or seamounts on the lower plate (2001 Peru event: Robinson *et al.* 2006; Das and Watts 2009), with structural features of the upper plate (1960 Valdivia, Chile, event: Melnick *et al.* 2009), or in general with the presence of irregularities and dip changes of the lower plate (*e.g.*, Vogt *et al.* 1976; Kelleher and McCann 1976). Fracture zones as both possible barriers and stress concentration points along the South America trench are briefly mentioned by Barrientos and Ward (1990) for the 1960 Valdivia earthquake. Bilek's (2009) extensive review of literature on the segmentation of the South American margin shows that most of the work has focused on finding features that act as barriers to rupture propagation.

Although the topic of control by lower-plate bathymetric features on worldwide subduction zone seismicity has been extensively covered, the issue of which features are significant for the nucleation of the largest events is still open. Here I examine the role played by oceanic fracture zones in controlling the initiation and extent of great and giant earthquakes along the South American trench. I will argue that bathymetric steps across fracture zones (Figure 3) play a major role and are equivalent in geometry and behavior to lateral ramps on continental thrust faults (Figure 4).

I focus on the six events mentioned above because for these at least a partial instrumental record exists, but I also consider older events to verify consistency of rupture patterns for each segment of the subducting plate. Throughout the paper I will continue to refer to M_w ~8.5 events with the understanding that it means any event with reported magnitude of 8.3 or higher. This is done in order to guarantee the inclusion of all events with M_w 8.5, accounting both for the variability in reported M_w for some instrumental events, and for the different methods used to convert other magnitudes to M_w for historical events.

LOWER-PLATE TOPOGRAPHY

Besides the observation above that the largest six earthquakes along this trench in the last 100 years nucleated near an oceanic fracture zone, the next relevant observation is that the 11 major fracture zones on the Nazca plate separate crust with ages different enough (Figure 1; Müller *et al.* 1997) to result in different depths of the sea floor. The changes in average seafloor depth across these fracture zones are also evident in the bathymetry map of Sandwell and Smith (1997; shown in Figure 2), and in published bathymetric profiles (*e.g.*, the Grijalva fracture zone; see Figure 3 adapted from Rea and Malfait 1974). For the Nazca plate (Figure 1), the expected offsets across the various fracture zones are several hundred meters to more than one kilometer (Parsons and Sclater 1977), consistent with the seafloor depth values from the Sandwell and Smith (1997) data. While direct imaging of such steps in the thrust seismogenic zone itself is problematic (it requires full onshore, high-resolution, 3D seismic imaging reaching depths of up to 35 km), there is no reason to believe that these steps would suddenly disappear once the Nazca plate enters the trench.

Only four out of 11 of the fracture zones of the Nazca plate are also associated with a submarine ridge, which can add up to 1.5 km of localized relief. Great and giant earthquakes have occurred both in the presence and absence of such ridges. In particular, the 1960 Valdivia and the 2010 Maule event hypocenters (Figure 5) were located near fractures with no associated ridges, suggesting that while ridges can contribute to the nucleation of great earthquakes (the 1906 M_w 8.8 Ecuador-Colombia earthquake epicenter was located near the Carnegie ridge; Kelleher 1972; Kanamori and McNally 1982), they are

doi: 10.1785/gssrl.82.5.629

TABLE 1

List of great and giant subduction earthquakes along the South America trench, 1500–2010. Due to the uncertainties in magnitude determination, I include all earthquakes starting at reported magnitude of 7.7 to avoid missing possible great earthquakes. For the northern Peru seismic gap, two smaller events are listed (in italics) to show at what magnitude the records start. Reported magnitude is M_w for post-1900 events. For older events, the magnitude reported varies. Even if the equivalent M_w has been calculated and reported for most of the older events, significant variations in reported magnitude for the same event are possible. The sources cited were also used for epicenter locations (where reported), and detailed information about uncertainties in locations can be found in these sources.

Event Location	Year	M	Sources of Epicenter Locations, Rupture and Magnitude Estimates
Peru	1513	≥7.7	Comte and Pardo, 1991
Tarapaca, Peru	1543	≥7.7	Comte and Pardo, 1991
Concepcion, Chile	1570	~8.0	Beck *et al.*, 1998; Lomnitz, 2004
Valdivia, Chile	1575	~8.5	Lomnitz, 2004; Cisternas *et al.*, 2005
Arequipa, Peru	1582	7.9–8.0	Comte and Pardo, 1991
Lima, Peru	1586	8.1	Dorbath *et al.*, 1990
Peru	1604	~8.7–9.0	Dorbath *et al.*, 1990; Comte and Pardo, 1991
Arica, Peru	1615	7.5–7.9	Comte and Pardo, 1991
Trujillo, Peru*	1619	7.7–8.0	Dorbath *et al.*, 1990
Concepcion, Chile	1657	~8.0	Beck *et al.*, 1998; Lomnitz, 2004
central Peru	1678	7.7–8.0	Dorbath *et al.*, 1990
Lima, Peru	1687	8.0	Dorbath *et al.*, 1990; Comte and Pardo, 1991
Lima, Peru	1687	8.4	Dorbath *et al.*, 1990
Peru-Chile	1715	7.8	Dorbath *et al.*, 1990; Comte and Pardo, 1991
Valparaiso, Chile	1730	8.5–9.0	Beck *et al.*, 1998; Lomnitz, 2004
Lima, Peru	1746	~8.6–9.2	Dorbath *et al.*, 1990
Concepcion, Chile	1751	8.5	Beck *et al.*, 1998; Lomnitz, 2004
southern Peru	1784	8.4–8.6	Dorbath *et al.*, 1990; Comte and Pardo, 1991
Copiapo, Chile	1819	8.5	Beck *et al.*, 1998; Lomnitz, 2004
Valparaiso, Chile	1822	8–8.5	Beck *et al.*, 1998; Lomnitz, 2004
Concepcion, Chile	1835	8–8.5	Beck *et al.*, 1998; Lomnitz, 2004
Valdivia, Chile	1837	8–8.5	Lomnitz, 2004; Cisternas *et al.*, 2005
Lima, Peru	1868	8.8–9.2	Dorbath *et al.*, 1990; Comte and Pardo, 1991; Okal *et al.* 2006
Iquique, Chile	1877	~8.8	Comte and Pardo, 1991; Lomnitz, 2004
Ecuador-Colombia	1906	8.8	Kelleher, 1972; Kanamori and McNally, 1982; Collot *et al.*, 2004
Valparaiso, Chile	1906	8.3–8.6	Beck *et al.*, 1998; Lomnitz, 2004
Chile-Argentina	1922	8.4	Beck *et al.*, 1998; Lomnitz, 2004
Talca, Chile	1928	7.8–8.4	Beck *et al.*, 1998; Lomnitz, 2004
central Peru	1940	7.8–8.2	Beck and Ruff, 1989; Dorbath *et al.*, 1990
central Peru	1942	8.1	Dorbath *et al.*, 1990; Swenson and Beck, 1996
Ecuador	1942	7.8–7.9	Collot *et al.*, 2004
Illapel, Chile	1943	7.9–8.3	Beck *et al.*, 1998; Lomnitz, 2004
Colombia	1958	7.7–7.8	Kanamori and McNally, 1982; Mendoza and Dewey, 1984
northern Peru	1960	7.6	Bilek, 2009
Valdivia, Chile	1960	7.8	Moreno *et al.*, 2009
Valdivia, Chile	1960	9.5	Moreno *et al.*, 2009
central Peru	1966	8.1–8.2	Dorbath *et al.*, 1990
northern Peru	1970	7.8	Beck and Ruff, 1989
central Peru	1974	7.8–8.1	Beck and Ruff, 1989; Giovanni *et al.*, 2002
Colombia-Ecuador	1979	8.1	Kelleher, 1972; Kanamori and McNally, 1982
central Chile	1985	8.0	Beck *et al.*, 1998; Bilek, 2009
northern Chile	1995	8.0	Beck *et al.*, 1998; Bilek, 2009
northern Peru	1996	7.5	Ihmle *et al.*, 1998
Nazca ridge, Peru	1996	7.7	Swenson and Beck, 1999
Lima, Peru	2001	8.4	Giovanni *et al.*, 2002; Robinson *et al.*, 2006
central Peru	2007	8.0	Bilek, 2009
northern Chile	2007	7.7	Bilek, 2009
Maule, Chile	2010	8.8	US Geological Survey, 2010

* It is not certain whether this was a subduction event.

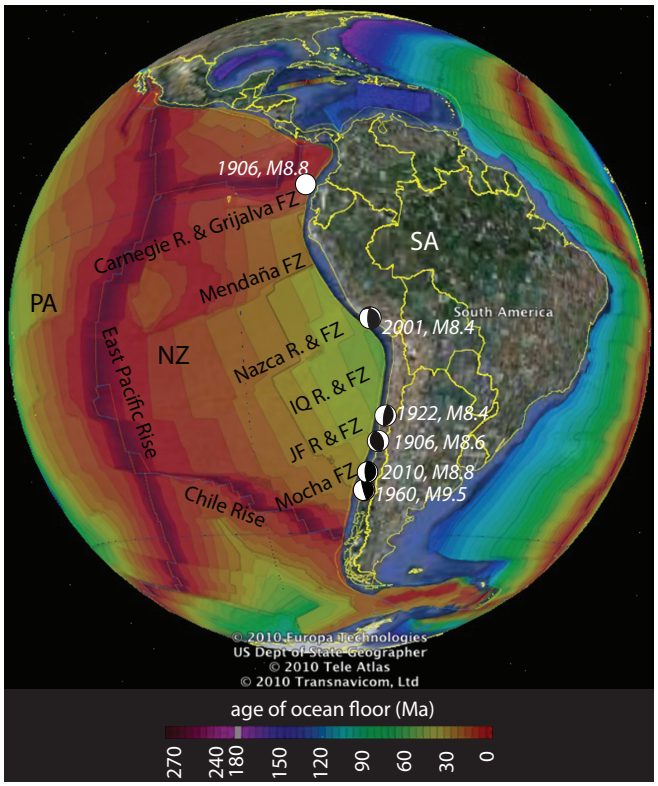

▲ **Figure 1.** Ages of ocean floor for the Nazca plate (from Müller *et al.* 1997). Major fracture zones (FZ) and ridges (R), shown together with the locations of six subduction earthquakes of M_w ~ 8.3 and larger that have occurred since 1900. The southernmost five fracture zones are named in Figure 5. The epicenter of each is near a major fracture zone or ridge on the subducting plate. Focal plane solutions indicated where available; otherwise a white circle indicates the epicenter. JFR = Juan Fernandez ridge, IQR = Iquique Ridge, PA = Pacific, NZ = Nazca, SA = South America.

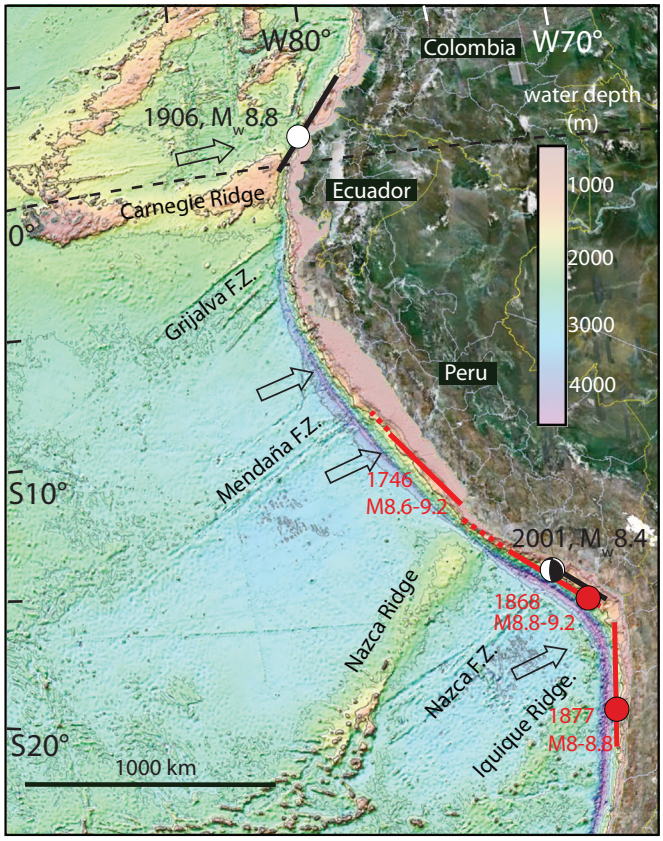

▲ **Figure 2.** Bathymetric map from Sandwell and Smith (1997). Changes in seafloor depth across each named feature are evident even from quick visual inspection: colors in 2,500–3,000 m range for Grijalva-Mendaña segment, in 3,000–3,500 m for Mendaña-Nazca, and to over 3,500 m between Nazca fracture zone and Iquique ridge. Red lines and circles indicate rupture length of well-documented M_w ~ 8.5 and larger pre-1900 events. Arrows indicate MORVEL direction of motion of the Nazca plate with respect to South America (DeMets *et al.* 2010), which can be used as a proxy for long-term slip direction on the subduction interface.

not a necessary condition, whereas a sustained step in the lower plate topography likely is.

The topography of the lower plate can be described as a thrust fault with large-scale lateral ramps (steps) subparallel to the long-term slip vector (block diagram in Figure 6). Because the average depth of the seafloor changes relatively quickly across fracture zones compared to the adjacent "flat" segments (Figure 3), lateral ramps are steep compared to the in-between segments. Ramps are not necessarily vertical "walls" however. The vertical steps in Figure 6 are mostly due to insufficient resolution: their tops and bottoms can be located anywhere in a 50–100 km range on either side of the step.

The subduction interface also has local, limited irregularities due to seamounts, smaller fracture zones, etc., but these do not produce any significant ramps perpendicular to the slip direction below depths of less than 100 km. At greater depth, there are slab tears and dip changes (Gutscher *et al.* 1999; Barazangi and Isacks 1976; Cahill and Isacks 1992), but these are below the region where megathrust earthquakes can nucleate, which is less than ~50 km depth for the South American margin (Tichelaar and Ruff 1991). Lateral ramps are thus the best candidates for nucleation of great and giant earthquakes along this margin.

THRUST LATERAL RAMPS AS SOURCES OF GREAT AND GIANT SUBDUCTION EARTHQUAKES

Nucleation of rupture at a thrust lateral ramp has been observed before: the 1994 **M** 6.8 Northridge, California, earthquake, for which both the detailed thrust geometry (Carena and Suppe 2002) and the rupture initiation and propagation (Wald *et al.* 1996) are well-constrained, shows slip propagating updip and away from the lateral ramp on the thrust (Figure 4). The hypocenter is located at one edge of the ramp and at the brittle-ductile transition, and the initial rupture coincides with the hypocenter.

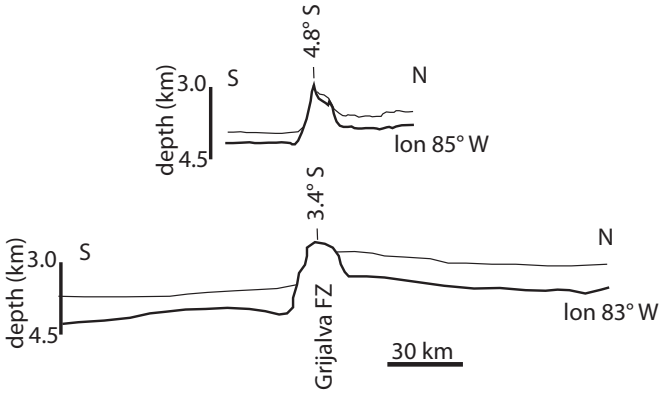

▲ **Figure 3.** Bathymetric profiles at two different longitudes across the Grijalva fracture zone (after Rea and Malfait 1974). From north to south across the fracture zone, the sea floor steps down more than 500 m. Thin line = top of sediments, thick line = top of basement.

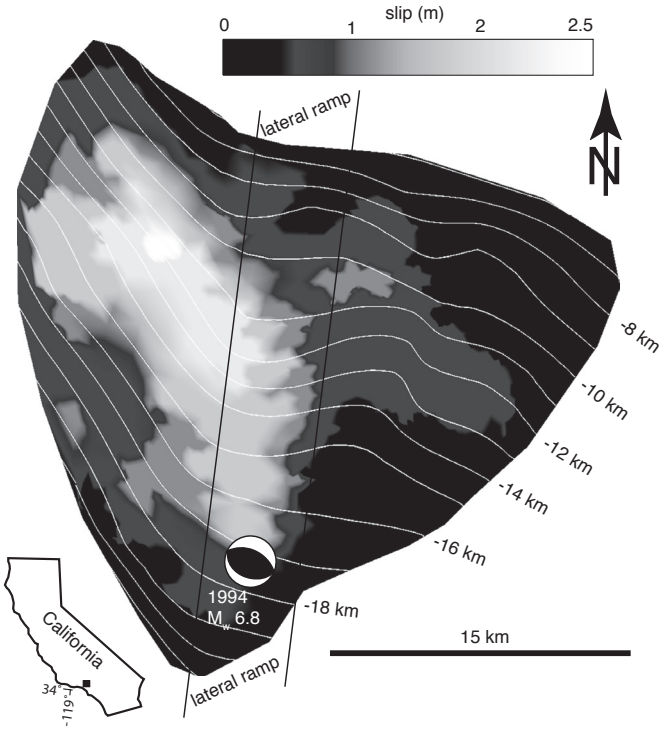

▲ **Figure 4.** Map view of the Northridge thrust (Carena and Suppe 2002) with the coseismic slip distribution (Wald *et al.* 1996) of the 1994 M_w 6.8 Northridge earthquake. The mainshock occurred on the thrust ramp, near the brittle-ductile transition depth, and the slip propagated updip and to the west, with very little slip occurring east of the ramp.

Lateral ramps on thrust faults are an obvious location for stress concentration and increased mechanical coupling. The maximum shear stress on a subduction thrust is near the brittle-ductile transition, at the base of the seismogenic zone (Sibson 1982; Tse and Rice 1986; Das and Scholz 1983). This is reflected in the depth range of the hypocenters of the great earthquakes along the South American trench. Any irregularities of the thrust surface, however, will produce stress concentrations (Scholz 1990), *i.e.*, an increase in mechanical coupling on the interface. One reason for increased coupling at lateral ramps is the increased contact area per unit length of strike of the thrust due to the ramp itself, plus any ridge on top of it. Additional stress concentration can also occur when the ramp is not perfectly parallel to the thrust slip direction and is thus closer to a jog than a step. The Mocha ramp (Figures 5 and 6), where the latest great earthquake nucleated, is an example of the latter. Increased mechanical coupling at a ramp means that, compared to the adjacent flat, the ramp will be stronger and fail at higher stresses. With plate convergence velocity being equal, flats may therefore reach failure earlier than adjacent ramps. In the long term, cumulative displacement on the flat must be the same as on the adjacent ramps, suggesting that, on average, ramps should nucleate events that have longer recurrence intervals and thus larger slip involving their whole down-dip width.

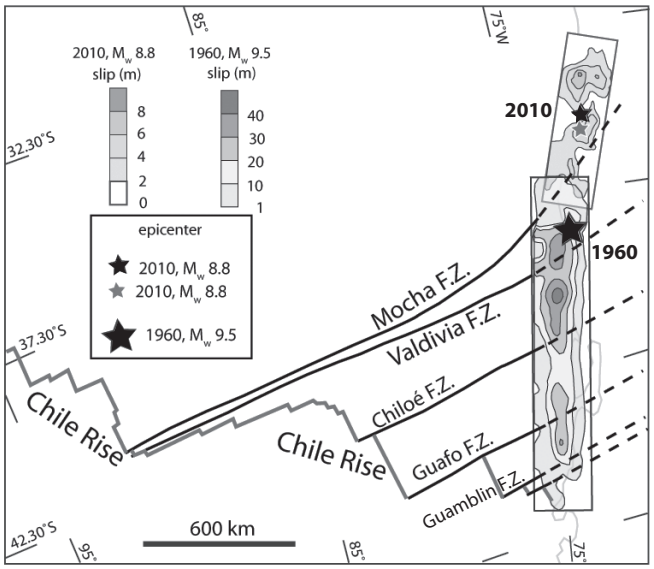

▲ **Figure 5.** Slip contour maps for the 2010 Maule event (simplified from Sladen 2010) and for the 1960 Valdivia event (simplified from Moreno *et al.* 2009). Small black star: epicenter location from Sladen (2010); small gray star: epicenter location from USGS (2010)

The more persistent a feature is on the topography of the thrust footwall, the more significant its influence will be. Lateral ramps in the megathrust topography are persistent in both dip and strike directions. Oceanic fracture zones extend for thousands of kilometers and cross the entire plate in the thrust dip direction. Given the 15°–20° average dip of the shallow part of the Nazca plate, this corresponds to a distance of up to 150–200 km within the locked seismogenic zone. Also, a step-up or step-down at a ramp is maintained along the topographic trench for hundreds to thousands of kilometers, until the next ramp. Ridges may have more relief than steps associated with fracture zones, but they are also narrow in the trench-parallel direction. Isolated seamounts are narrow in both directions and, at the plate scale and earthquake sizes considered, are usually not significant enough to either nucle-

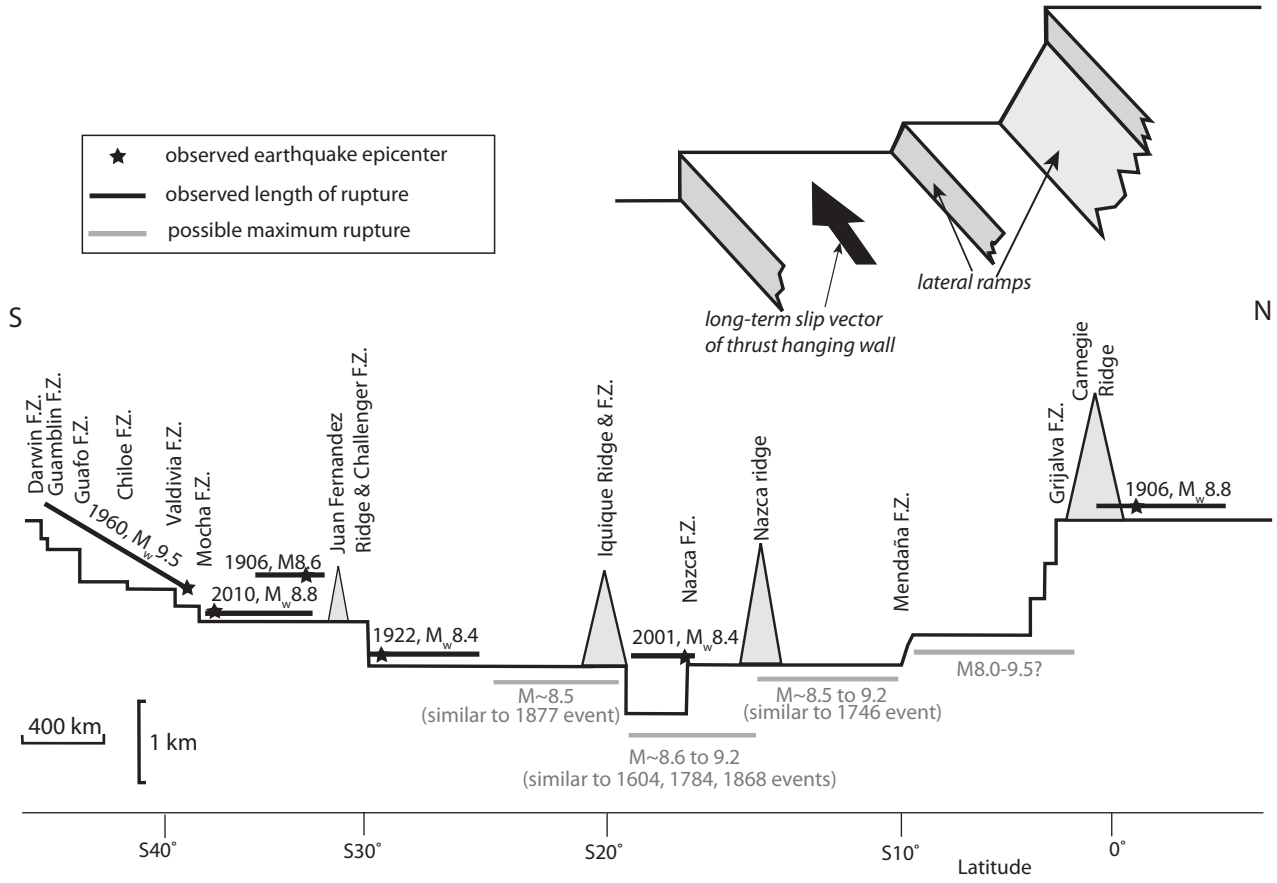

▲ **Figure 6.** Trench-parallel schematic profile (bottom) and 3D schematic view (top right) of lower-plate topography. Fracture zones form steps 100 to 1,400m high (note 400x vertical exaggeration) on the basement of the subducting oceanic plate. In some places, ridges are associated with them. The long-term slip vector of the subduction thrust is subparallel to the trend of most of these features. The six instrumental earthquakes shown (black stars) have started close to a lateral ramp. The gaps that remain could be filled by similar earthquakes also originating at lateral ramps (gray lines). As in Figure 7, latitude is measured parallel to trench at intersection between subducted feature and the subduction thrust.

ate large ruptures, or impede rupture propagation (Scholz and Small 1997). Seamounts and discontinuous ridges can in principle be sheared off at their base when certain conditions are met (Cloos 1992; Das and Watts 2009). In contrast, because a lateral ramp spans the width of the seismogenic zone and the elevation change of the thrust footwall persists along strike, a rupture cannot simply go around it as it could with smaller obstacles. Similarly, the ramp cannot be permanently sheared off, so the rupture must climb it to keep propagating.

GREAT AND GIANT EARTHQUAKE RUPTURES ALONG THE SOUTH AMERICAN TRENCH

At this point it is necessary to examine the entire record of subduction thrust events along the South American trench to determine whether their spatial pattern is compatible with the observations made about the distribution of instrumental events and with the lateral ramp hypothesis. Figure 7 shows that, although great earthquakes with magnitude below ~8.5 have also occurred in the middle of a segment bounded by fracture zones, larger ones always start at the edge of a segment and propagate toward its interior, and can span multiple segments. For those events where epicenter latitude (stars in Figure 7) is reasonably well-known, the epicenter is less than 100 km from a fracture zone or from the edge of a ridge in all (100%) of the eight events with **M** larger than ~8.5, but only in eight (50%) of the 16 smaller events. Also, rupture propagation is mostly unidirectional (100% of larger events and 80% of smaller ones). There are no instances on record of earthquakes with M_w < ~8.5 that break across a fracture zone. These events are either confined within a segment or, in the presence of a ridge, can break part or the entire ridge but not continue into the ridge-free part of the segment.

Once a great earthquake nucleates, the rupture propagates generally upward toward the trench and away from the ramp (Scholz 1990). All six instrumental events considered nucleated at depths shallower than 50 km (Tichelaar and Ruff 1991; USGS 2010). Unilateral rupture is clear in the 1960 (Barrientos and Ward 1990; Moreno *et al.* 2009) and 2001 Peru events (Robinson *et al.* 2006; Das and Watts 2009), and likely for the 1922 (Beck *et al.* 1998) and 1906 Ecuador-Colombia events (Kelleher 1972).

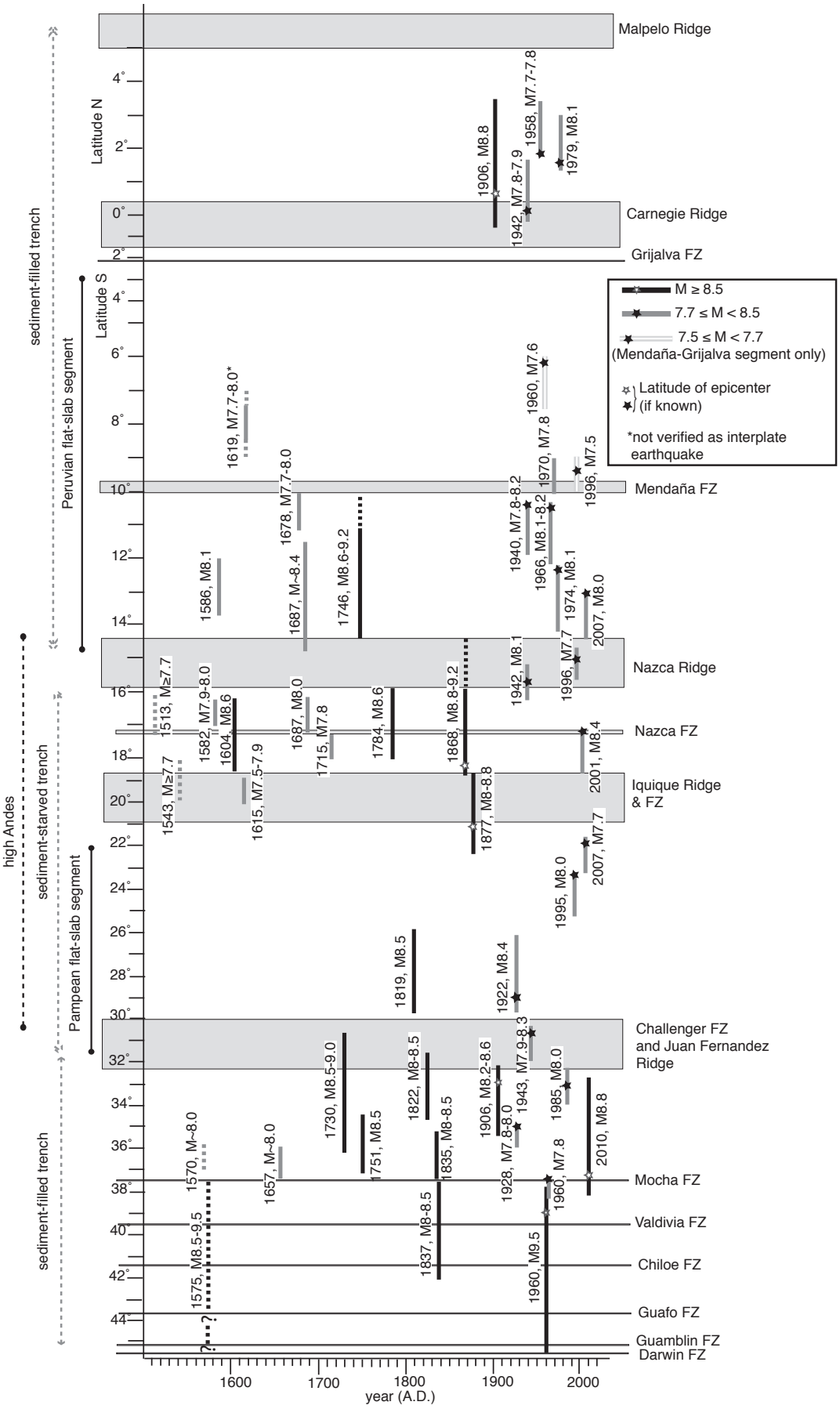

▲ **Figure 7.** Space and time distribution of great and giant earthquakes. Events above **M** ~ 7.7 are considered because of uncertainties and variability in methods used, especially for pre-instrumental events. **M** = M_w for most, but not all, events. For some pre-1900 events M_w has never been estimated. The range of **M** given for individual events in the figure thus reflects both the different estimates of M_w given by different authors and the fact that for a few older events no M_w value is available. The epicenter locations (stars) are the most likely locations as reported by the sources cited in Table 1 for each event. The latitude of lineaments like ridges or fracture zones (FZ) is taken at the intersection between the subduction thrust seismogenic zone and the landward projection of the lineament, rather than at the intersection between lineament and trench. This is based on the rationale that the location of the lineament on the subduction interface is related to earthquake nucleation. Spacing of degrees of latitude on axis is variable because it reflects distances measured parallel to trench rather than along a meridian.

The best evidence is for the recent M_w 8.8 event offshore Maule, which started at the Mocha fracture zone and propagated mostly northward, stopping near the Juan Fernandez ridge, but also southward (preliminary slip models by USGS 2010 and Sladen 2010). However, the southern propagation does not cross the Mocha ramp, as can be shown by considering the 3D geometric relationships between fracture zone, thrust surface, and earthquake hypocenter. In map view, the Mocha fracture zone curves and enters the trench at an angle of ~60° (Figure 5). The hypocenter must then be located near the northern base of the ramp, which would not be the case if the fracture zone had been straight. The curvature of the fracture zone also has the consequence that, because most of the slip to the south occurred updip from the hypocenter (Figure 5), the earthquake ruptured both the thrust north of the ramp and part of the ramp itself, but very little of the slip propagated south past the ramp. This could explain the slower southern propagation observed by Sladen (2010). Therefore the 2010 event started near a ramp and propagated mostly away from it.

DISCUSSION AND CONCLUSIONS

Whether a rupture climbs the next ramp encountered during propagation or not (*i.e.*, whether the next ramp will act as a barrier, or whether the earthquake will continue rupturing and further increase in magnitude) depends upon how much energy has already been dissipated when this ramp is reached. A thrust lateral ramp requires the rupture to step up or down and continue along the next large segment of the thrust. In a thrust event, the propagating rupture is a mode III crack relative to a lateral ramp. The necessary driving stress to step over the ramp depends both on the height of the ramp and on its inclination with respect to the plane of the thrust (Scholz 1990). If most of the elastic energy has been dissipated by the time the rupture encounters the ramp, the crack will not be able to step across it coseismically, making the ramp a barrier to this event. Instead of coseismic rupture propagation, the stepover to the next segment may happen in a later event due to static stress triggering. Increased Coulomb stress is predicted for unbroken thrust segments that have the same orientation as an adjacent one that broke (*e.g.*, the 1994 Northridge earthquake, Stein 1999; and the 2003 San Simeon earthquake, Aron and Hardebeck 2009). Where ramps are closely spaced, it is more likely that a rupture will arrive with enough energy to step across another ramp coseismically. This could be the case for the 1960 event, which started at the Valdivia fracture zone and propagated south across the Chiloe, Guafo, and Guanblin fracture zones (Barrientos and Ward 1990; Moreno *et al.* 2009). This sequence of steps was likely also followed in the 1575 event (Cisternas *et al.* 2005). It is worth noting that, compared to the rest of the margin farther north, these fracture zones have no associated ridge and their ramp heights are smaller (mostly less than 200 m) and the in-between flat segments shorter (300 km or less). In addition, this section of the trench is filled with sediments, which have also been implicated in controlling the size of subduction earthquakes (Ruff 1989). Conversely, the segments between ramps along the trench north of the Mocha fracture zone are longer (up to over 1,000 km for the segment between the Iquique ridge and the Juan Fernandez ridge, Figure 6), so it is more likely that the rupture will stop before reaching the next ramp. In fact, no single earthquake appears to have completely ruptured the segment between the Juan Fernandez and Iquique ridges. The largest earthquakes on record (1877 and 1922, Figure 7) ruptured only the northern and southern halves. The 2001 M_w 8.4 Peru earthquake started near the top of the Nazca fracture zone lateral ramp, climbed down the ramp, and broke also the adjacent flat segment, stopping at the Iquique ridge ramp. This propagation is described by Robinson *et al.* (2006), who also observe the rupture briefly stalling on the Nazca ramp before stepping down.

These observations concerning $M_w \sim 8.5$ and larger events along the South American trench let us make some predictions about which lateral ramps may nucleate a significant rupture in the near future. Three ramp-flat regions have not fully broken in a single event for the last 100 years: the Grijalva-Mendaña (northern Peru), the Mendaña-Nazca (central Peru), and the stretch between 21° and 26° south of the Iquique ridge (central Chile; Figure 7). Of these, only the Mendaña-Nazca has at least one pre-1900 event on record that hints at the size of possible future earthquakes: the 1746 event, which ruptured the whole segment with M_w 8.6–9.2 (Figure 7). The Iquique ridge zone could generate an M_w 8.5–8.8 event, similar to the one of 1877 (Figure 7), though a much larger event could rupture all the way south to the Juan Fernandez ramp.

The Grijalva-Mendaña segment appears to have had no great earthquakes in the past 500 years: the largest reported event is M_w 7.6 (Figure 7). However, due to its geometry and by comparison with the other segments, it is in principle capable of producing earthquakes above M_w 9 if a rupture started at either end. A question is whether the Grijalva-Mendaña segment is mostly creeping and hence will not have very large events, or locked, in which case it might produce one of the largest earthquakes to occur along the South American trench.

It has been suggested that the absence of great earthquakes on this segment may be related to subduction occurring by aseismic creep possibly due to a "flat slab" associated with subduction of the Carnegie ridge (McCann *et al.* 1979) or the thickness of sediment fill in the trench (Ruff 1989). Figures 2 and 7 offer several insights. First, the Colombia-Ecuador segment to the north and the central Chile segment to the south also have rather low seismicity levels. Second, northern Peru, like central Peru, has a flat slab and a sediment-filled trench, but central Peru has more evenly distributed great earthquakes. Third, central Chile is also underlain by a flat slab, but the trench is sediment-starved. Thus, there seems to be no obvious correlation between the size and frequency of great earthquakes, and slab dip or trench fill along the South American trench.

Another observation is that for the Ecuador-Colombia segment the handful of great earthquakes on record are limited to the last 100 years, and in central Chile the great earthquakes recorded are all in the last 200 years (Figure 7). Anyone looking at the Ecuador-Colombia segment before 1900, or at the

central Chile segment before 1800, might have concluded that these segments creep aseismically.

Thus these three "low seismicity" segments may simply have a 500-year recurrence cycle for $M_w \geq 8.5$ events, with the Grijalva-Mendaña segment in northern Peru nearing the end of a cycle, and the other two segments being closer to the middle of a cycle. The need for records longer than the available historical ones has been highlighted by Stein and Okal (2007) for the Sumatra region, where the giant earthquake of 2004 and the great earthquakes that followed were unexpected due to the short earthquake history available. In fact, the earthquake record for the Grijalva-Mendaña segment is similar to that of northern Sumatra (Bilham *et al*. 2005; Satake and Atwater 2007) in having no M_w 8 events in the historical record and just three events above M_w 7.5. This segment also shows the same characteristics (age < 80 Ma, convergence rate between 30 and 70 mm/yr) of other subduction zones where giant earthquakes have occurred (Stein and Okal 2007).

In conclusion, only a paleoseismological record significantly longer than the historically available 500 years (towns like Chiclayo and Trujillo in northern Peru were founded after the year A.D. 1500) and adequate geodetic observations would tell whether the typical long-term behavior of the Grijalva-Mendaña segment is aseismic creep, or infrequent (>500-year period) giant earthquakes followed by clusters of great earthquakes. Similarly long records would be needed to understand the long-term behavior of the Ecuador-Colombia and the central Chile segments.

ACKNOWLEDGMENTS

The author thanks Seth Stein and an anonymous reviewer for their constructive comments.

REFERENCES

Aron, A., and J. L. Hardebeck (2009). Seismicity rate changes along the central California coast due to stress changes from the 2003 **M** 6.5 San Simeon and 2004 **M** 6.0 Parkfield earthquakes. *Bulletin of the Seismological Society of America* **99**, 228–229; doi:10.1785/0120080239.

Barazangi, M., and B. L. Isacks (1976). Spatial distribution of earthquakes and subduction of the Nazca plate beneath South America. *Geology* **4**, 686–692.

Barrientos, S., and S. N. Ward (1990). The 1960 Chile earthquake: Inversion for slip distribution from surface deformation. *Geophysical Journal International* **103**, 589–598.

Beck, S., S. Barrientos, E. Kausel, and M. Reyes (1998). Source characteristics of historic earthquakes along the central Chile subduction zone. *Journal of South American Earth Sciences* **11**, 115–129.

Beck, S. L., and L. J. Ruff (1989). Great earthquakes and subduction along the Peru trench. *Physics of the Earth and Planetary Interiors* **57** (3–4), 199–224.

Bilek, S. L. (2007). Influence of subducting topography on earthquake rupture. In *The Seismogenic Zone of Subduction Thrust Faults*, ed. T. H. Dixon and J. C. Moore, 123–146. New York: Columbia University Press.

Bilek, S. L. (2009). Seismicity along the South American subduction zone: Review of large earthquakes, tsunamis, and subduction zone complexity. *Tectonophysics* doi:10.1016/j.tecto.2009.02.037.

Bilham, R., R. Engdahl, N. Feldl, and S. P. Satybala (2005). Partial and complete rupture of the Indo-Andaman plate boundary 1847–2004. *Seismological Research Letters* **76,** 299–311.

Cahill, T., and B. L. Isacks (1992). Seismicity and shape of the subducted Nazca plate. *Journal of Geophysical Research* **97**, 17,503–17,529.

Carena, S., and J. Suppe (2002). Three-dimensional imaging of active structures using

earthquake aftershocks: The Northridge thrust, California. *Journal of Structural Geology* **24**, 887–904.

Cisternas, M., B. F. Atwater, F. Torrejon, Y. Sawai, G. Machuca, M. Lagos, A. Eipert, C. Youlton, I. Salgado, T. Kamataki, M. Shishikura, C. P. Rajendran, J. K. Malik, Y. Rizal, and M. Husni (2005). Predecessors of the giant 1960 Chile earthquake. *Nature* **437**, 404–407; doi:10.1038/nature03943.

Cloos, M. (1992). Thrust-type subduction zone earthquakes and segment asperities: A physical model for seismic rupture. *Geology* **20**, 601–604.

Collot, J. Y., B. Marcaillou, F. Sage, F. Michaud, W. Agudelo, P. Charvis, D. Graindorge, M. Gutscher, and G. Spence (2004). Are rupture zone limits of great subduction earthquakes controlled by upper plate structures? Evidence from multi-channel seismic reflection data acquired across the northern Ecuador-southwestern Colombia margin. *Journal of Geophysical Research* **109**, B11103.

Comte, D., and N. Pardo (1991). Reappraisal of great historical earthquakes in the northern Chile and southern Peru seismic gaps. *Natural Hazards* **4**, 23–44.

Das, S., and C. H. Scholz (1983). Why large earthquakes do not nucleate at shallow depths. *Nature* **305**, 621–623.

Das, S., and A.B. Watts (2009). Effects of subducting seafloor topography on the rupture characteristics of great subduction zone earthquakes. In *Subduction Zone Geodynamics*, ed. S. Lallemand and F. Funiciello, 103–118. Berlin: Springer. doi:10.1007/978-3-540-87974-9.

De Mets, C., R. G. Gordon, and D.F. Argus (2010). Geologically recent plate motions. *Geophysical Journal International* **181**, 1–80; doi:10.1111/j.1365-246x.2010.04491.x.

Dorbath, L., A. Cisternas, and C. Dorbath (1990). Assessment of the size of large and great historical earthquakes in Peru. *Bulletin of the Seismological Society of America* **80**, 551–578.

Giovanni, M. K., S. L. Beck, and L. Wagner (2002). The June 23, 2001 Peru earthquake and the southern Peru subduction zone. *Geophysical Research Letters* **29** (21); doi:10.1029/2002GL015774.

Gutscher, M.-A., J. Malavieille, S. Lallemand, and J.-Y. Collot (1999). Tectonic segmentation of the North Andean margin: Impact of the Carnegie ridge collision. *Earth and Planetary Science Letters* **168**, 255–270.

Ihmle, P. F., J. M. Gomez, P. Heinrich, and S. Guibourg (1998). The 1996 Peru tsunamigenic earthquake: Broadband source process. *Geophysical Research Letters* **25** (14), 2,691–2,694.

Kanamori, H., and K. C. McNally (1982). Variable rupture model of the subduction zone along the Ecuador-Colombia coast. *Bulletin of the Seismological Society of America* **72** (4), 1,241–1,253.

Kelleher, J. (1972). Rupture zone of large South American earthquakes and some predictions. *Journal of Geophysical Research* **77**, 2,087–2,103.

Kelleher, J., and W. McCann (1976). Buoyant zones, great earthquakes, and unstable boundaries of subduction. *Journal of Geophysical Research* **81**, 4,885–4,896.

Lomnitz, C. (2004). Major earthquakes of Chile: A historical survey, 1535–1960. *Seismological Research Letters* **75**, 368–378.

Mendoza, C., and J. W. Dewey (1984). Seismicity associated with the great Colombia-Ecuador earthquakes of 1942, 1958, and 1979: Implications for barrier models of earthquake rupture. *Bulletin of the Seismological Society of America* **74** (2), 577–593.

McCann, W. R., S. P. Nishenko, L. R. Sykes, and J. Krause (1979). Seismic gaps and plate tectonics: Seismic potential for major boundaries. *Pure and Applied Geophysics* **117**, 1,082–1,147.

Melnick, D., B. Bookhagen, M. R. Strecker, and H. P. Echtler (2009). Segmentation of megathrust rupture zones from fore-arc deformation patterns over hundreds to millions of years, Arauco peninsula, Chile. *Journal of Geophysical Research* **114**, B01407; doi:10.1029/2008JB005788.

Mogi, K. (1969). Relationship between the occurrence of great earthquake and tectonic structures. *Bulletin of the Earthquake Research Institute* (University of Tokyo) **47**, 429–451.

Moreno, M. S., J. Bolte, J. Klotz, and D. Melnick (2009). Impact of megathrust geometry on inversion of coseismic slip from geodetic data: Application to the 1960 Chile earthquake. *Geophysical Research Letters* **36**, L16310; doi:10.1029/2009GL039276.

Müller, R. D., W. R. Roest, J.-Y. Royer, L. M. Gahagan, and J. G. Sclater (1997). A digital age map of the ocean floor. *Journal of Geophysical Research* **102**, 3,211–3,214.

Okal, E. A., J. C. Borrero, and C. E. Synolakis (2006). Evaluation of tsunami risk from regional earthquakes at Pisco, Peru. *Bulletin of the Seismological Society of America* **96** (5), 1,634–1,648; doi:10.1785/0120050158.

Parsons, B., and J. G. Sclater (1977). An analysis of the variation of ocean floor bathymetry and heat flow with age. *Journal of Geophysical Research* **82**, 803–827.

Rea, D. K., and B. T. Malfait (1974). Geologic evolution of the northern Nazca plate. *Geology* **2**, 317–320.

Robinson, D. P, S. Das, and A. B. Watts (2006). Earthquake rupture stalled by a subducting fracture zone. *Science* **312**, 1,203–1,205.

Ruff, L. J. (1989). Do trench sediments affect great earthquake occurrence in subduction zones? *Pure and Applied Geophysics* **129**, 263–282.

Sandwell, D. T., and W. H. F. Smith (1997). Marine gravity anomaly from Geosat and ERS1 satellite altimetry. *Journal of Geophysical Research* **102**, 10,039–10,054.

Satake, K., and B. F. Atwater (2007). Long-term perspectives on giant earthquakes and tsunamis at subduction zones. *Annual Reviews of Earth and Planetary Sciences* **35**, 349–374.

Scholz, C. (1990). *The Mechanics of Earthquakes and Faulting*. Cambridge: Cambridge University Press, 439 pp.

Scholz, C. H., and C. Small (1997). The effect of seamount subduction on seismic coupling. *Geology* **25**, 487–490.

Sibson, R. E. (1982). Fault zone models, heat flow, and the depth distribution of seismicity in the continental crust of the United States. *Bulletin of the Seismological Society of America* **72**, 151–163.

Sladen, A. (2010). Slip maps for recent large earthquakes: M_w 8.8 Maule, Chile; http//tectonics.caltech.edu/slip-history/2010-chile/index.html. Last accessed 3/19/2010.

Stein, R. S. (1999). The role of stress transfer in earthquake occurrence. *Nature* **402**, 605–609.

Stein, S., and E. A. Okal (2007). Ultralong period seismic study of the December 2004 Indian Ocean earthquake and implications for regional tectonics and the subduction process. *Bulletin of the Seismological Society of America* **97**, S279–S295, doi:10.1785/0120050617.

Swenson, J. L., and S. L. Beck (1996). Historical 1942 Ecuador and 1942 Peru subduction earthquakes, and earthquake cycles along Colombia-Ecuador and Peru subduction segments. *Pure and Applied Geophysics* **146** (1), 67–101.

Tichelaar, B. T., and L. J. Ruff (1991). Seismic coupling along the Chilean subduction zone. *Journal of Geophysical Research* **96**, 11,997–12,022.

Tse, S., and J. Rice (1986). Crustal earthquake instability in relation to the depth variation of frictional slip properties. *Journal of Geophysical Research* **91**, 9,452–9,472.

U.S. Geological Survey (USGS) (2010). Earthquake database; http://earthquake.usgs.gov/earthquakes/. Last accessed 4 March 2010.

Vogt, P., A. Lowrie, D. Bracey, and R. Hey (1976). *Subduction of Oceanic Aseismic Ridges: Effects on Shape, Seismicity, and Other Characteristics of Consuming Plate Boundaries*. Geological Society of America Special Paper 172. Boulder, CO: Geological Society of America, 59 pp.

Wald, D. J., T. S. Heaton, and K. W. Hudnut (1996). The slip history of the 1994 Northridge, California, earthquake determined from strong ground motion, teleseismic, GPS and leveling data. *Bulletin of the Seismological Society of America* **86**, 549–570.

Department of Earth and Environmental Sciences
University of Munich
Luisenstraße 37, 80333
Munich, Germany
scarena@iaag.geo.uni-muenchen.de